Structure Determination of the Cyclohexene Ring of Retinal in Bacteriorhodopsin by Solid-State Deuterium NMR†

Anne S. Ulrich,‡ Maarten P. Heyn,§ and Anthony Watts*,‡

Department of Biochemistry, University of Oxford, South Parks Road, Oxford OX1 3QU, U.K., and Department of Physics, Freie Universität Berlin, Arnimallee 14, 1000 Berlin 33

Received January 22, 1992; Revised Manuscript Received July 28, 1992

ABSTRACT: The orientation and conformation of retinal within bacteriorhodopsin of the purple membrane of *Halobacterium halobium* was established by solid-state deuterium NMR spectroscopy, through the determination of individual chemical bond vectors. The chromophore ([2,4,4,16,16,16,17,17,17,18,18-$^2H_{11}$]retinal) was specifically deuterium-labeled on the cyclohexene ring and incorporated into the protein. A uniaxially oriented sample of purple membrane patches was prepared and measured at a series of inclinations relative to the spectrometer field. ^{31}P NMR was used to characterize the mosaic spread of the oriented sample, and computer simulations were applied in the analysis of the ^2H NMR and ^{31}P NMR spectral line shapes. From the deuterium quadrupole splittings, the specific orientations of the three labeled methyl groups on the cyclohexene ring could be calculated. The two adjacent methyl groups (on C_1) of the retinal were found to lie approximately horizontal in the membrane and make respective angles of 94° ± 2° and 75° ± 2° with the membrane normal. The third group (on C_5) points toward the cytoplasmic side with an angle of 46° ± 3°. These intramolecular constraints indicate that the cyclohexene ring lies approximately perpendicular to the membrane surface and that it has a (6*S*)-trans conformation. From the estimated angle of the tilt of the chomophore long axis, it is concluded that the polyene chain is slightly curved downward to the extracellular side of the membrane.

To understand fully the mechanistic details of the function of a protein, it is necessary to establish its detailed three-dimensional structure, paying particular attention to the active site and any associated prosthetic groups. For membrane proteins, whose amphipathic nature makes crystallization inherently difficult, alternative structural approaches to diffraction methods have to be developed. Multidimensional high-resolution NMR[1] (nuclear magnetic resonance) analysis of protein structure is only successful when the molecules tumble so rapidly as to average out all anisotropic line-broadening interactions, which is the case for small (≤20 kDa) soluble proteins. In biological membranes, however, the constituent lipids and proteins undergo relatively slow and highly restricted motions on the time scale of the NMR experiment. This anisotropy causes extensive broadening and overlapping of the lines, but these broad characteristic line shapes may be examined by solid-state NMR methods. Particularly in combination with selective isotope labeling, solid-state NMR provides a powerful tool to characterize the structural and dynamic properties of biomembranes (Smith & Oldfield, 1984; Lugtenburg et al., 1988; Griffin et al., 1988; Opella, 1990; Shon et al., 1991). In a macroscopically oriented membrane sample, specifically placed deuterons can be used as nonperturbing reporters for the geometry of the labeled site within the protein. From the spectral quadrupole splitting, the individual chemical bond vector of the deuterated group can be determined (Lee & Oldfield, 1982). Complementary neutron diffraction experiments can be performed on the same deuterated sample to localize the depth of the labeled group within the bilayer. The combined information thus provides a comprehensive description of the local protein structure and will lead to a better understanding of its function in the membrane.

We present a strategy for determining the structure of a prosthetic group within a membrane protein by deuterium (^2H) NMR, using bacteriorhodopsin (BR) as a well-characterized model system (Mathies et al., 1991). The protein is arranged as a planar array throughout the purple membrane (PM) of *Halobacterium halobium*, which grows in concentrated brine. Under conditions of oxygen starvation, the protein acts as a light-driven proton pump to generate an electrochemical gradient across the membrane, which is utilized in the synthesis of ATP. The retinal chromophore, which is linked to Lys-216 through a protonated Schiff base, undergoes an all-trans to 13-cis isomerization upon the absorption of light. During the photocycle, a transient deprotonation of the Schiff base is involved in transferring a proton across the membrane. Knowledge of the detailed geometry and orientation of the retinal chromophore and its interaction with the surrounding amino acid residues is thus essential for the elucidation of protein function.

Retinal is buried within the seven membrane-spanning α-helices of the protein, and it is attached to helix G as shown in the cartoon in Figure 1. The three-dimensional structure of BR has recently been determined by electron microscopy to a resolution of 2.7 Å in-plane and 10 Å vertically (Henderson et al., 1990; Ceska & Henderson, 1990). The electron density map reveals the position of the cyclohexene ring of retinal within the protein, but its orientation and conformation are not yet fully discernible. By neutron scattering, the positions of individual deuterium-labeled segments along the chromophore could be located in-plane as well as across the membrane, and thus the three-dimensional orientation of the retinal long axis within the protein could be established (Seiff

† This work was supported by the EC, SERC Grants GR/F/69400, GR/F/80852, and GR/E/69188 (to A.W.), and an SERC studentship (to A.S.U.).

* Corresponding author.
‡ University of Oxford.
§ Freie Universität Berlin.

[1] Abbreviations: ^2H NMR, deuterium nuclear magnetic resonance; BR, bacteriorhodopsin; PM, purple membrane; CSA, chemical shielding anisotropy; FWHH, full width at half-height.

0006-2960/92/0431-10390$03.00/0

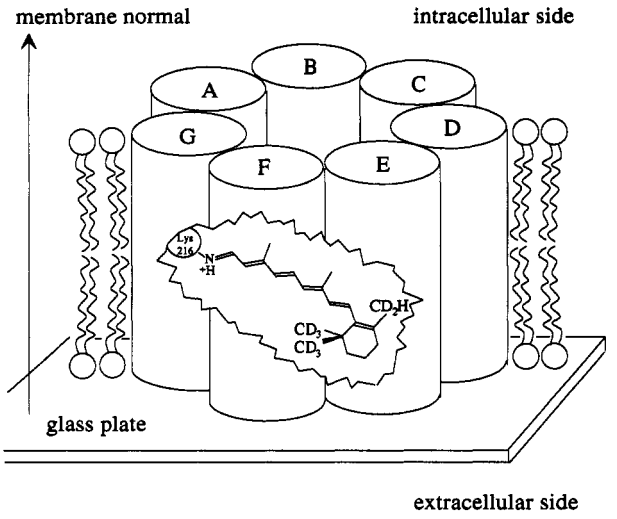

FIGURE 1: Retinal chromophore in BR is attached via a protonated Schiff base to Lys-216 on helix G and is tilted toward the extracellular side. To determine its detailed structure, retinal was selectively deuterated on the three methyl groups on the cyclohexene ring and incorporated into BR from *H. halobium*. The PM patches were deposited as uniaxially oriented films on small glass plates by evaporation and were then dark-adapted. ^{2}H NMR analysis yielded the bond vectors of the three deuteromethyl groups, which thus define the structure of the cyclohexene ring of the chromophore.

et al., 1986, 1987; Heyn et al., 1988; Hauss, et al., 1990). A variety of spectroscopic techniques has been used to obtain detailed information about the structure of retinal within BR, as shown in Figure 1. The tilt angle of the chromophore long axis (which was assumed to be parallel to the electronic transition moment) was determined to be about 67° relative to the membrane normal (Heyn et al., 1977; Korenstein & Hess, 1978; Bamberg et al., 1979; Barabas et al., 1983; Earnest et al., 1986; Urabe et al., 1989; Lin & Mathies, 1989; Schertler et al., 1991), with the molecular plane of the polyene chain aligned approximately vertical (Earnest et al., 1986; Urabe et al., 1989; Lin & Mathies, 1989). Retinal was found to be tilted away from Lys-216 toward the extracellular side (Huang et al., 1982; Huang & Lewis, 1989), with the methyl groups along the polyene chain pointing toward the cytoplasmic side of the membrane. The proton on the Schiff base nitrogen faces the extracellular side (Lin & Mathies, 1989; Hauss et al., 1990), both in the light- and dark-adapted state of the protein (Smith et al., 1984; Harbison et al., 1984a). Retinal is generally accepted to assume a (6*S*)-trans conformation in BR (Harbison et al., 1985; van der Steen et al., 1986; Smith et al., 1989; Copie et al., 1990; Creuzet et al., 1991), unlike the (6*S*)-*cis*-retinal in the visual rhodopsins or retinal in solution.

In this paper, we describe a novel approach to obtain structural information on the chromophore of BR from ^{2}H NMR spectroscopy [for preliminary results see Ulrich and Watts (1991)]. An essential aspect of this new approach is the use of anisotropic samples, in which the labeled purple membrane patches are oriented at a well-defined angle with respect to the magnetic field. From a spectral analysis of the quadrupole splittings of deuterated methyl groups on the chromophore, the orientations of these methyl rotors may be obtained. In order to establish the feasibility of the method and in view of the low sensitivity of NMR, we have used a strongly labeled chromophore with the three methyl groups on the cyclohexene ring deuterated. Because of the spectral overlap resulting from this choice, computer line shape simulation was performed to aid the spectral analysis, but this does not constitute an essential step for the study of individual labeled methyl groups. All structural conclusions that could be derived from the determination of the three bond vectors in this study are consistent with the recognized orientation and conformation of retinal in BR. These experiments therefore provide a promising foundation for further investigation of other deuterated sites on the chromophore or elsewhere in the protein, under a variety of conditions relevant in the photocycle of bacteriorhodopsin.

MATERIALS AND METHODS

Sample Preparation and Spectroscopy. Retinal was specifically deuterated on the cyclohexene ring as described (Seiff et al., 1986, 1987). The synthetic [2,4,4,16,16,16,-17,17,17,18,18-$^2H_{11}$]retinal contains three labeled methyl groups, i.e., two CD_3 groups on C_1 and one CD_2H group on C_5 (see Figure 1). The three methylene deuterons on C_2 and C_4 do not contribute to the ^{2}H NMR spectrum due to their relaxation behavior and are not shown. The deuterated molecule was incorporated into BR using a mutant of *H. halobium* that is deficient in the synthesis of retinal (Seiff et al., 1986, 1987), and the PM was harvested and purified. Oriented membrane films were prepared by slowly (over 48 h) evaporating a concentrated suspension of the labeled PM patches in ^{2}H-depleted water on glass plates cut from microscope cover slips. In this way, uniaxial films with good orientation of the purple membrane patches parallel to the plates are obtained (Seiff et al., 1987). A total of about 90 mg of BR (corresponding to 25 μmol of deuterons) was distributed over the surface of 18 small plates (8 mm × 30 mm × 0.15 mm, or 5 mm × 30 mm × 0.15 mm), which were then assembled into a parallel stack that was fitted longitudinally into a 10-mm NMR tube. The films were typically 50 μm thick, and the humidity was maintained within the closed tube by a saturated KCl solution. The dark-adapted sample could be rotated within the horizontal solenoid, allowing the angle between the plates and the magnetic field to be set with a precision of ±3°. After completion of all oriented experiments, the viscous PM films were scraped off their supports and tightly packed into an NMR tube, for the acquisition of randomly oriented powder spectra. All ^{2}H NMR spectra were acquired on a Bruker MSL 400 spectrometer at a deuterium frequency of 61 MHz, using a quadrupole-echo pulse sequence with a $\pi/2$ pulse width of 5 μs, echo delay times around 20–30 μs, and a repetition time of 100–200 ms. The ^{31}P NMR was performed on a Bruker MSL 200 spectrometer at a phosphorus frequency of 81 MHz with ^{1}H decoupling, using a single pulse with a $\pi/2$ width of 4 μs, echo delay times around 30 μs, and a repetition time of 1.3 s. To minimize artifacts in detection, all NMR measurements employed the standard quadrature phase cycling provided in the Bruker software.

Solid-State ^{2}H NMR of Oriented Samples. The power of this method lies in the ability to determine the orientation of a specifically labeled molecular segment relative to the symmetry axis of a macroscopically aligned sample. A simple anisotropic ^{2}H NMR spectrum is characterized by a pair of lines corresponding to the two transitions allowed for the deuterium nucleus with a spin of $I = 1$. The quadrupole splitting $\Delta\nu_Q$ depends on the angle θ between the deuterium bond vector in the molecule and the magnetic field direction $\vec{H}$ (Seelig, 1977; Lee & Oldfield, 1982; Smith & Oldfield, 1984; Griffin et al., 1988). For a rapidly spinning methyl group, the direction of the three individual deuterium bonds

is time averaged, and the effective bond vector described by θ is that of the methyl rotor axis. The resulting segmental order parameter, S_{CD3}, reduces the quadrupole splitting corresponding this one particular methyl group to

$$\Delta\nu_Q = [3(e^2qQ/h)/2]S_{CD3}[(3\cos^2\theta - 1)/2]$$
$$= \Delta\nu_{powder}(3\cos^2\theta - 1) \quad (1)$$

where $\Delta\nu_{powder}$ = 40 kHz at –60 °C (39 kHz at room temperature), as determined from the splitting in the powder pattern of the labeled PM. Using the specified delay times in the ^{2}H NMR echo experiment, immobile methylene deuterons do not show up due to their relaxation properties. It is therefore possible to take advantage of mobile groups, such as deuteromethyl rotors, as reporters for this structural method.

Solid State ^{31}P NMR. The phosphorus nucleus with a spin $I = {}^1/_2$ has a chemical shielding anisotropy (CSA) tensor which is axially symmetric in the case of phospholipids undergoing fast rotation in the fluid bilayer. Therefore, any one type of phosphorus in an oriented membrane sample gives rise to a single line in the ^{31}P NMR spectrum. The resonance position ν (expressed in parts per million relative to the isotropic frequency) varies with the angle α between the membrane normal and the magnetic field direction $\vec{H}$ (Seelig, 1978):

$$\nu = \Delta\nu_{CSA}(3\cos^2\alpha - 1)/3 \quad (2)$$

where $\Delta\nu_{CSA}$ corresponds to the full width of the phosphorus powder pattern.

Uniaxially Oriented Membranes. The preparation of uniaxially oriented samples is fundamental to this ^{2}H NMR approach. There are various alternatives to the method described above to achieve macroscopic alignment of membrane proteins, such as squeezing dispersions between glass plates (Seelig, 1977), magnetic or electric orientation (Lee & Oldfield, 1982; Shon et al., 1991), or centrifugation (Clark et al., 1980). Whether an individual membrane fragment settles face up or face down onto the support is immaterial for the NMR analysis, since both cases yield the same spectrum. Figure 2 illustrates the geometry within such an immobilized and uniaxially oriented PM sample, placed into the spectrometer with an inclination α of the sample normal $\vec{N}$ relative to the magnetic field direction $\vec{H}$. There is no translational or rotational symmetry within the plane of the sample, due to the azimuthally random stacking of the membrane patches around the sample normal $\vec{N}$, as is well known from the X-ray diffraction pattern of such films. For a perfectly oriented sample, all deuterium bond vectors $\vec{D}$ of any one type lie uniformly along the rim of a cone around the sample normal $\vec{N}$, with a well-defined angle γ (see Figure 2). In the case of a time-averaged deuteromethyl group, $\vec{D}$ corresponds to its rotor axis. The spectrum of such a deuteromethyl group recorded with a horizontal sample, i.e., at an inclination of $\alpha = 0°$, simply consists of a pair of lines, with a quadrupole splitting determined by the cone angle γ. Since there are three geometrically distinct deuteromethyl groups on the labeled retinal in BR, three pairs of lines are expected, each with a quadrupole splitting that is related to the respective methyl rotor axis. Using eq 1 (with $\theta = \gamma$), it should be straightforward to calculate the three cone angles γ from the values of $\Delta\nu_Q$ and thus determine the structure of the cyclohexene ring in BR.

Unfortunately, for the evaluation of γ it is not necessarily sufficient to determine the quadrupole splitting from a horizontally oriented sample, because positive and negative

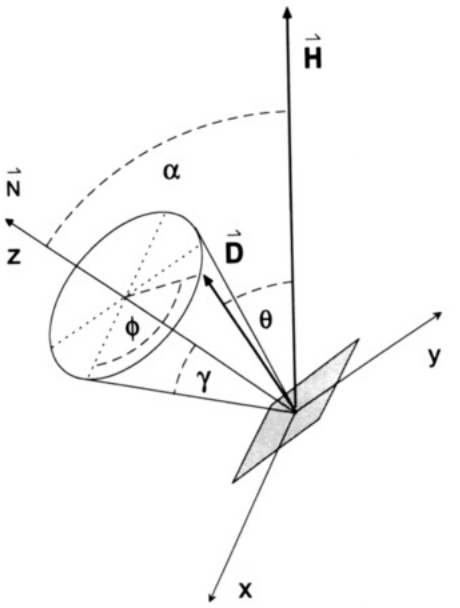

FIGURE 2: Uniaxially oriented sample on a glass plate (shaded area) shown at an inclination α relative to the spectrometer magnetic field $\vec{H}$. All immobilized deuterium bond vectors (or deuteromethyl rotors) $\vec{D}$ of any one type lie uniformly along the rim of a cone with angle γ around the membrane normal $\vec{N}$. This axis coincides with the sample normal for the case of perfect orientation (zero mosaic spread), and it is defined parallel to the z-axis of the coordinate system which was used in the derivation of eq 3 describing the ^{2}H NMR spectral line shape. The spherical polar coordinates of $\vec{D}$ are γ (fixed) and ϕ, and one particular vector $\vec{D}$ is shown making an angle θ with $\vec{H}$. All $\vec{D}$ vectors contribute to the spectrum and ϕ is taken from 0° through to 360°. The corresponding variation in the value of θ, which determines the quadrupole splitting (eq 1), leads to the complex line shape of eq 3.

signs of $\Delta\nu_Q$ cannot be discriminated. This introduces a 2-fold redundancy across ${}^2/_3$ of the possible spectral range, as there exist two angles, on either side of the magic angle (54.7°), which correspond to the same absolute value of $\Delta\nu_Q$. This redundancy, however, is removed at sample inclinations other than $\alpha = 0$ in the magnetic field, because the different molecular geometries would now give rise to distinctly differing line shapes. Note that this characteristic feature does not apply to fluid systems such as lipid molecules or small membrane proteins that are motionally averaged around the sample normal on the ^{2}H NMR time scale ($\tau_c < 10^{-6}$ s). For immobilized samples, positive and negative values of $\Delta\nu_Q$ can be discriminated and the unique solution found for γ, by measuring a tilt series of the oriented sample at several discrete angles between 0° and 90° or at least one additional spectrum at the extreme vertical sample inclination. The line shapes for $\alpha \neq 0$ are considerably more complex than the simple picture for a horizontal sample outlined above, because any one cone of bond vectors will now contribute a range of resonances to the ^{2}H NMR spectrum with a continuous spread of splittings. Such line shapes have received little attention in theoretical analysis or practical application to molecular structure, so we have developed a simulation program to aid the interpretation of the tilt series acquired for the oriented BR sample. A general illustration and discussion of the ^{2}H NMR line shape variation as a function of sample inclination will be published later (Ulrich et al., manuscript in preparation).

Computer Line Shape Simulation Program. The simulation of NMR line shapes from tilted sampled provides an inductive approach to spectral analysis and helps in the

discrimination between positive and negative values of $\Delta\nu_Q$. Moreover, line shape simulation provided a means of resolving the overlapping resonances in the ^2H NMR spectra of the labeled BR, which all happened to fall into a relatively narrow spectral range.

Mathematically, the simulation program is based on the calculation of the probability density $p(\zeta)$ as a function of the reduced resonance frequency ζ, which describes the intensity envelope of the spectral line shape. Such line shapes have been computed for the investigation of molecular dynamics in uniaxially oriented samples (Vaz et al., 1984), but in the static case considered here the asymmetry parameter is assumed to be zero. Thus the line shape equation was derived for either of the two nuclear spin transitions ζ_+/ζ_-, where each curve is bound by two singularities which vary as a function of α and γ. The total spectral line shape is given by the sum $p(\zeta) = p(\zeta_+) + p(\zeta_-)$, with

$$p(\zeta_\pm) \propto \frac{1}{\sqrt{\frac{\pm 2\zeta_\pm + 1}{3}}\sqrt{\sqrt{\frac{\pm 2\zeta_\pm + 1}{3}} - \cos(\alpha + \gamma)}\sqrt{\cos|\alpha - \gamma| - \sqrt{\frac{\pm 2\zeta_\pm + 1}{3}}}} \quad (3)$$

The angles are defined in Figure 2. Angle ϕ is used only in the derivation of $p(\zeta_\pm)$, where it is taken through 0–360° to cover the full range of deuterium vectors along the cone. Note that for the limit of $\gamma = 90°$, which corresponds to a flat radial distribution of bond vectors, eq 3 reduces to the simple expression derived by Seelig (1977) for the case of oriented lipid cylinders in the hexagonal H_{II} phase.

In the simulation of NMR line shapes, spectral line broadening effects have to be taken into account which can be attributed to two distinct sources, namely, the intrinsic line width of the NMR transition and the mosaic spread of the macroscopically oriented sample. The effective intrinsic line width, defined as the full width at half-height (FWHH), is due to the limited lifetime of a spin transition as well as field inhomogeneities. This line broadening contribution is included in the simulation program as a constant Lorentzian broadening over all orientations. The assumption of approximately isotropic spin–spin relaxation times T_2^* seemed justified by the good line fit of the simulated powder patterns across the whole spectral width. The mosaic spread is defined as the standard angular deviation (in degrees) of the aligned PM patches in a macroscopically oriented sample. The line shape calculation takes the mosaic spread contribution into account by summing up a series of line shapes that were generated for a range of angles around the selected value of α, using a Gaussian distribution for the weighting of their relative intensities. As the simulation program was developed for the complex line shapes of immobilized uniaxially oriented samples, it is necessarily also applicable to other more simple oriented systems, such as motionally averaged lipid bilayers (where $\gamma = 0°$) and hexagonal lipid systems (where $\gamma = 90°$).

Strategy of Line Shape Simulation. The basic line shape of an oriented ^2H NMR spectrum is described by the mathematical expression in eq 3, which depends on the parameters α and γ alone. Since the sample inclination α in the magnet is set in the experiment, the unknown quantity that determines the spectral line shape is the cone angle γ, which is directly related to the molecular geometry. An unambiguous spectral analysis can be achieved by line shape simulation of a series of oriented spectra, as only the correct choice of γ will give a good line fit throughout the whole data set. The labeled BR contains three methyl rotors, each of which is characterized by a specific but as yet unknown angle γ. The three bond vectors are rigidly connected to one another via the cyclohexene ring, with an underlying tetrahedral geometry. This tetrahedral symmetry is due to the stiffness of the $C_5{=}C_6$ double bond, which retains the CD_2H group parallel to the C_1–C_6 bond. Therefore, all three vectors on the deuterated molecular unit have to be considered simultaneously in the simulation procedure, and their resonance positions in the ^2H NMR spectrum are interdependent. Note that they contribute different intensities to the total spectrum, according to the number of deuterons on the methyl rotor.

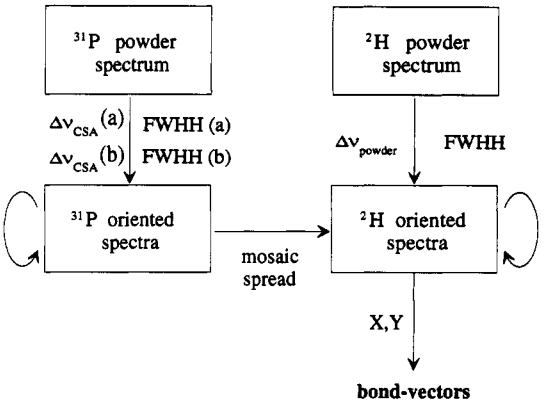

FIGURE 3: Flowchart showing the strategy used in the simulation analysis of the NMR spectra. From the ^{31}P and the ^2H powder patterns, values representative of the full spectral width ($\Delta\nu_{CSA}$ or $\Delta\nu_{powder}$, respectively) and the intrinsic line widths (FWHH) were found, and the mosaic spread was then deduced from the additional broadening of the ^{31}P NMR spectra. Hence, in the concerted simulation of the oriented ^2H NMR spectra, only the rotation angles X and Y needed to be optimized, which lead to the desired geometry of the deuterated molecular unit.

Consider the orientations of the three deuteromethyl groups within the membrane, expressed as unit vectors in a Cartesian coordinate system defined with its z-axis parallel to the sample normal. The starting positions for the three tetrahedrally connected unit vectors were conveniently defined as CD_3(a) = $\{-1,-1,-1\}/\sqrt{3}$, CD_3(b) = $\{-1,1,1\}/\sqrt{3}$, and CD_2H = $\{1,-1,1\}/\sqrt{3}$. This rigid set of vectors can be aligned in space with every possible orientation, by performing two rotations X and Y of the whole deuterated unit about the x- and the y-axis in the sample plane. These two variables are sufficient to cover all possible molecular orientations in the membrane, in view of the axial symmetry of the macroscopically oriented sample around the z-axis. In the simulation procedure, random line shapes are generated initially and compared with the experimental spectrum. The quality of the line fit is then improved by a concerted variation of X and Y and judged visually until the optimized line shape is obtained. The final choice of the rotations X and Y thus defines the orientations of the methyl groups on the cyclohexene ring within the protein.

When an unknown parameter such as the orientation of a bond vector is to be deduced by the simulation of oriented ^2H NMR spectra, it is crucial to ensure that the values of all other parameters used to generate the line shape are known and do not introduce further variability. In the analysis of the labeled retinal in BR, unique values for the two line broadening parameters can be evaluated independently from additional ^2H NMR and ^{31}P NMR data. This strategy is illustrated in Figure 3 and is based on the fact that the observed broadening in the powder pattern from an unoriented random sample is due solely to the intrinsic spectral line width and does not include any mosaic spread. The intrinsic line width (FWHH), together with a parameter representative of the full spectral width ($2 \times \Delta\nu_{powder}$, or $\Delta\nu_{CSA}$), can therefore be deduced from the powder pattern. These values are then

applied to the simulation of the spectra from the macroscopically oriented sample, and any additional broadening required for a good line fit is therefore representative of the mosaic spread. An independent evaluation of the mosaic spread of the oriented PM sample can be obtained by analyzing a series of ^{31}P NMR spectra of the phospholipid component in the same sample that was used for the ^{2}H NMR experiments. The flowchart in Figure 3 summarizes the complete process of first finding the values of the phosphorus intrinsic line width (FWHH) and the chemical shielding anisotropy ($\Delta\nu_{CSA}$) from the ^{31}P NMR powder pattern and then the mosaic spread from the set of oriented ^{31}P NMR spectra. The intrinsic deuterium line width (FWHH) and the full spectral width ($2 \times \Delta\nu_{powder}$) are each deduced from the ^{2}H NMR powder spectrum, and finally only the two rotation angles X and Y remain to be optimized in a concerted fitting procedure of the oriented ^{2}H NMR spectra (over five different sample inclinations). The spectrum recorded at $\alpha = 0°$ has the highest information content and the quality of line fit is judged most unambiguously. Therefore, this line shape [see Figures 4(ii) and 6] was used for the fine adjustment of the values X and Y and the determination of error limits.

RESULTS

^{2}H NMR Spectra of Oriented Membranes. Figure 4 shows representative experimental ^{2}H NMR spectra from the labeled retinal in BR in a dark-adapted PM sample. The line shape simulations that were generated in the data analysis (see below) are shown superimposed on the experimental spectra. The powder pattern [Figure 4(i)] serves as a general reference for the tilt series of spectra recorded at various sample inclinations [Figure 4(ii)], because it defines the accessible frequency region over which the spectral intensity can occur. The oriented sample was measured at every 22.5° between 0° and 90°, of which three inclinations are represented in Figure 4(ii) with $\alpha = 0°$, 45°, and 90°. With the sample aligned horizontally in the magnet, further spectra were recorded over a range of temperatures from 30 down to −120 °C. Representative line shapes are compared in Figure 4, for 21 °C (iii) and −60 °C (ii). The signal-to-noise ratio improves dramatically with decreasing temperature, and therefore the spectral analysis was based on the set of data acquired at −60 °C. The central resonance line which appears at temperatures above 0 °C is due to HDO. Two components appear to be resolved at 21 °C, but they are found to broaden out and merge to give the unresolved line shape at −60 °C. A possible interpretation of this observation could be that some small local fluctuations within the puckered cyclohexene ring are frozen out in a slight glassy disorder, which is commonly found in crystalline retinal derivatives (Stam, 1972; Santasiero et al., 1990). Nevertheless, the overall line shape does not change significantly over the whole range of temperatures examined, and therefore the structure of the chromophore appears to remain relatively unaffected by freezing. From neutron scattering also it was found that the position of deuterium labels on either end of the chromophore are the same at room temperature and at −188 °C (Hauss and Heyn, unpublished results).

The characteristic shape of the ^{2}H NMR powder pattern [Figure 4(i)] indicates that the dynamics of the rotating methyl groups lie within the fast-motional limit at temperatures down to −120 °C (Smith & Oldfield, 1984; Griffin et al., 1988; Copie et al., 1990). This assumption is further supported by the increasing signal-to-noise ratio with decreasing temperature, since no loss, but rather a gain, in intensity is observed on cooling (Beshah et al., 1987). It is also clear that the

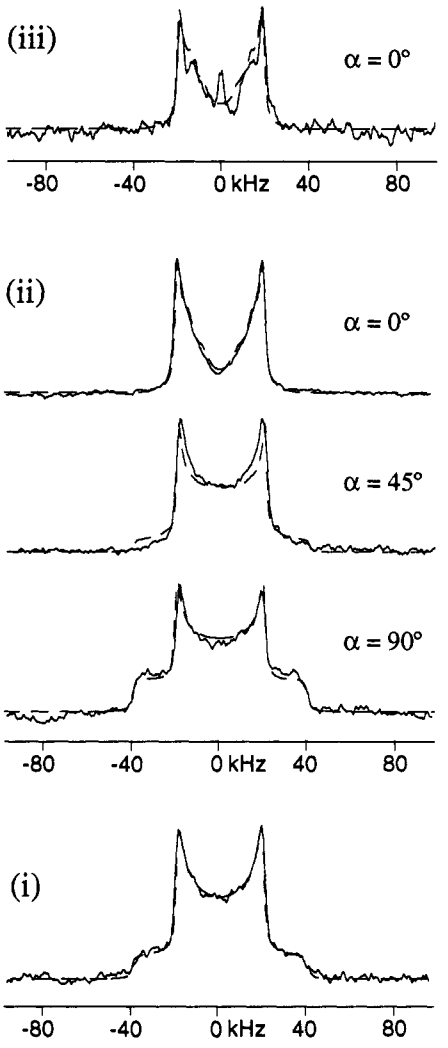

FIGURE 4: Representative ^{2}H NMR spectra (full lines) of dark-adapted BR (90 mg) containing deuterated retinal, with line shape simulations (dashed lines) superimposed. Both the powder spectrum (i) from randomly oriented PM patches and the tilt series (ii) over sample inclinations $\alpha = 0$, 45°, and 90°, were recorded at −60 °C (number of scans, 1.7×10^5, for $\alpha = 0°$). Spectrum (iii) was measured at 21 °C with $\alpha = 0°$ (number of scans, 3×10^5). All ^{2}H NMR spectra were recorded at 61 MHz, using a quadrupole-echo pulse sequence with a $\pi/2$ pulse width of 5 μs, echo delay times around 20–30 μs, and a repetition time of 100–200 ms.

cyclohexene ring does not undergo significant librational motion within its binding pocket, since the ^{2}H NMR spectra are not time-averaged by this type of random oscillation (with a correlation time $\tau_c < 10^{-6}$ s). The polyene chain of the chromophore has been shown to be completely immobilized on the time scale of 10^{-9}–10^{-2} s (Kouyama et al., 1981), indicating the absence of any rotational freedom.

With a horizontally oriented sample ($\alpha = 0°$), the spectrum of the labeled BR in Figure 4(ii) should display three quadrupole splittings corresponding to the three labeled methyl groups on the retinal. It is apparent, however, that the expected three pairs of resonances are not resolved because of spectral overlap of the broadened lines. A computer simulation approach was used to analyze the spectral line shapes despite the overlap (see below), but much qualitative information about the cyclohexene ring can be gained by simple inspection of the experimental data in Figure 4. From the spectra recorded at a sample inclination $\alpha = 0°$, it is concluded that none of the three deuteromethyl groups lies at an angle less than $\gamma = 35°$ relative to the sample normal, because there is no spectral intensity beyond ±20 kHz which would be the

region corresponding to cone angles $\gamma < 35°$ (eq 1, where $\theta = \gamma$). Furthermore, the lack of intensity in the central region of the same oriented spectrum indicates that cone angles around the magic angle ($\gamma = 54.7°$) are also excluded. Within the series of three different sample inclinations in Figure 4(ii), a recurring splitting of 40 kHz between the line shape maxima is noticed. A value for $\Delta\nu_{powder}$ of the same magnitude (40 kHz) is found in the powder pattern [Figure 4(i)], where it is simply due to the high statistical probability for a deuteromethyl group bond vector to occur at an effective angle $\theta = 90°$, regardless of the geometry within the molecule. In the oriented sample, however, which has a finite mosaic spread, the reason for the 40-kHz splitting must be the presence of a deuteromethyl group oriented approximately at a right angle ($\gamma = 90°$) relative to the membrane normal (eq 1). As outlined above, in principle there are actually two possible methyl rotor angles γ which would satisfy the splitting of 40 kHz in the oriented sample at $\alpha = 0°$, namely, $\gamma = 90°$ or $\gamma = 35°$. In case of the experimental ^{2}H NMR spectrum in Figure 4(ii), however, it is clear from the sharp edges of the line shape that the angle cannot be 35°, because any small mosaic spread would then cause a broadening of these edges beyond ±20 kHz. Therefore, one of the methyl groups on retinal in BR must be aligned at an approximately right angle to the membrane normal.

The spectrum measured at a sample inclination of $\alpha = 90°$ provides further evidence for methyl groups lying horizontally within the membrane. The relevant argument here follows from the line shape function (eq 3), but nevertheless the qualitative effect of the magnitude of γ on the line shape is readily demonstrated in the case of a vertical sample inclination ($\alpha = 90°$). In a cone of bond vectors $\vec{D}$ (see Figure 2) with an opening angle less than $\gamma = 90°$, i.e., anything other than a flat disk, not a single bond vector would be aligned parallel with the magnetic field $\vec{H}$. So for a vertical sample inclination, the smallest possible angle between $\vec{D}$ and $\vec{H}$ would be equal to $\theta = (90° - \gamma)$, and no intensity would be observed near the limits of the accessible spectral region where $\theta = 0°$. The edges in the experimental ^{2}H NMR spectrum measured at $\alpha = 90°$ in Figure 4(ii), however, extend right up to ±40 kHz, which are the extreme limits defined by the full spectral width of the powder pattern. Therefore, there must exist a population of methyl rotors aligned approximately horizontally within the membrane, as already proposed above. The remarkably high spectral intensity at these edges even suggests that this population is likely to consist of two rather than just one out of the three labeled methyl groups on the retinal. Once the orientations of two deuteromethyl groups have been fixed in space, the angle of the third one is automatically defined, because all rotors are rigidly connected to one another via the cyclohexene ring with a tetrahedral symmetry. In this first qualitative picture of retinal within BR, which has been obtained ab initio by ^{2}H NMR, two methyl groups are thus placed roughly horizontally in the membrane, and the third one is protruding at an angle consistent with the overall tetrahedral geometry of the deuterated cyclohexene unit. It should be noted that this simple analysis has not yet permitted the assignment of any of the methyl groups, which therefore leaves three possible ways of positioning the whole retinal molecule relative to the protein. However, only one of the three solutions is consistent with the quantitative simulation analysis and with the structural information about BR from spectroscopic and neutron diffraction studies (see later).

Sample Characterization by ^{31}P NMR. The mosaic spread of the macroscopically oriented PM sample that was used for the ^{2}H NMR experiments can be determined by ^{31}P NMR. This parameter is important in assessing the quality of alignment in the sample, and a numerical estimate of the mosaic spread is required for the line shape simulation analysis of the ^{2}H NMR spectra. The ^{31}P NMR powder pattern from an unoriented random PM sample is shown in Figure 5(i) and a tilt series of spectra from the macroscopically oriented system at five sample inclinations between $\alpha = 0°$ and 90° in Figure 5(ii). Best-fit line shape simulations are shown superimposed over each experimental spectrum. All spectra consist of two components a and b with an integrated intensity ratio around 1:1. These components correspond to the two phosphate groups in PGP (phosphatidylglycerophosphate), which is the principal phospholipid (85%) in native PM (Kates et al., 1982).

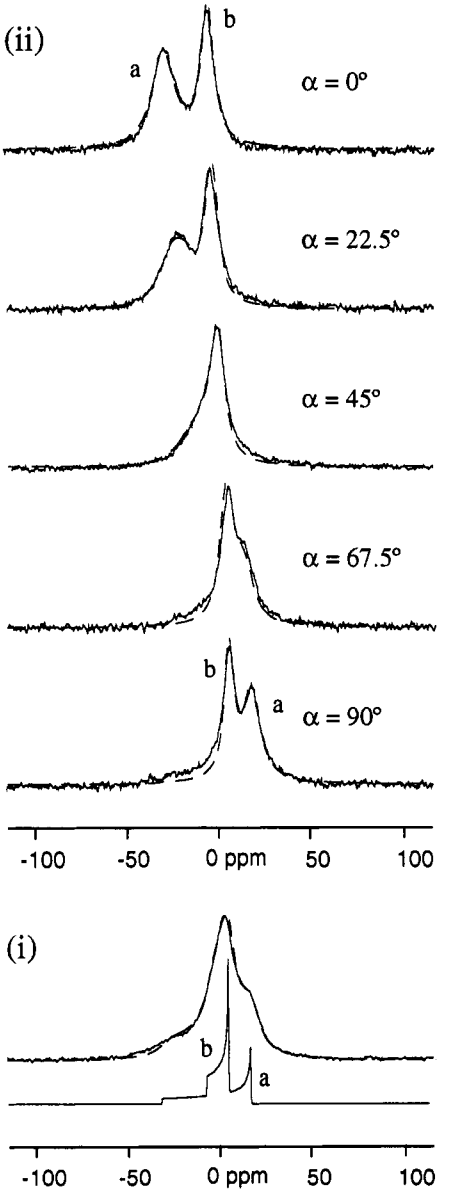

FIGURE 5: ^{31}P NMR spectra (solid lines) of the same PM sample that was used for the ^{2}H NMR experiments, with line shape simulations (dashed lines) superimposed. Below the experimental and simulated powder patterns (i), an equivalent line shape simulation is shown with a zero intrinsic line width to reveal the two spectral components (a and b) which correspond to the two phosphate groups in the principal PM phospholipid PGP (phosphatidylglycerophosphate). The tilt series (ii) was measured at sample inclinations α = 0°, 22.5°, 45°, 67.5°, and 90° in the magnetic field, at room temperature. All ^{31}P NMR spectra were recorded at 81 MHz with ^{1}H decoupling, using a single pulse with a $\pi/2$ width of 4 μs, echo delay times around 30 μs, and a repetition time of 1.3 s.

Line shape simulation of the ^{31}P NMR powder pattern was performed, assuming identical isotropic spectral origins for the two phosphate groups. The best line fit was obtained with the following values for the full spectral width ($\Delta\nu_{CSA}$) and the intrinsic line width (FWHH), in good agreement with previously determined data on PM (Ekiel et al., 1981):

$$\Delta\nu_{CSA}(a) = 53 \text{ ppm} \qquad \text{FWHH(a)} = 5.3 \text{ ppm}$$

$$\Delta\nu_{CSA}(b) = 13 \text{ ppm} \qquad \text{FWHH(b)} = 4.0 \text{ ppm}$$

The value of $\Delta\nu_{CSA}$ is characteristic of the geometry and motional averaging of the particular phosphate segment. Hence the spectral component a in Figure 5 can be assigned to the phosphodiester in the lipid backbone, which is expected to have a much larger $\Delta\nu_{CSA}$ than the terminal phosphate group giving rise to component b in Figure 5. Since the intrinsic line width (FWHH) is inversely proportional to the effective T_2^* relaxation time (in the fast motional regime), it is also clear from the values of a and b that the terminal phosphate segment b is less motionally restricted than the phosphodiester a. In order to illustrate how the two spectral components constitute the rather featureless appearance of the ^{31}P NMR powder pattern, the line shape simulation that is shown superimposed over the experimental spectrum in Figure 5(i) is repeated underneath, but with a zero intrinsic line width applied. Now, for each component a and b the characteristic angular dependence of a ^{31}P NMR resonance is apparent from the line shape, where the left and right edges correspond to the respective 0° and 90° orientations of the lipid molecules in the randomly oriented sample. This variation of the resonance position with angle (eq 2) is illustrated by the tilt series of the oriented ^{31}P NMR spectra in Figure 5(ii) over five sample inclinations (α = 0°, 22.5°, 45°, 67.5°, and 90°). Each of the two components gives rise to a single broadened line which traverses its accessible frequency region (defined by the respective $\Delta\nu_{CSA}$) from left to right with progressive sample inclination, with a crossover at the magic angle (α = 54.7°). From the broadening in this set of line shapes, the mosaic spread of the macroscopically oriented PM sample can now be deduced by simulation, using the appropriate values of $\Delta\nu_{CSA}$ and FWHH that were established above. A mosaic spread of ±10° was found to produce the best line fits, which is somewhat larger than the value (±6°) determined by neutron diffraction (Heyn et al., 1988) for an oriented sample prepared in the same way.

^2H NMR Simulation Results. The computational approach presented here allows a more thorough and accurate interpretation of the ^2H NMR data than the qualitative arguments outlined above. The powder pattern of the deuterated BR in Figure 4(i) has a quadrupole splitting between the line shape maxima of $\Delta\nu_{powder}$ = 40 kHz at –60 °C (39 kHz at room temperature) and simulation analysis yielded an intrinsic deuterium line width of 2 kHz (FWHH). Using this value together with the mosaic spread of ±10° as determined by the ^{31}P NMR spectral simulations, line shapes could be generated for any combination of the two rotations X and Y of the deuterated molecular unit, to be compared with the experimental data. The concerted optimization over the series of oriented spectra (α = 0°, 22.5°, 45°, 67.5° and 90°) yielded the best-fit line shapes, which are shown superimposed over the experimental spectra in Figure 4(ii). These simulations are based on the unique set of rotation angles $X = -33° \pm 2°$ and $Y = 9° \pm 3°$, which thus define the orientation of the deuterated unit in space. Only the mirror image to the corresponding structure constitutes another solution to the line fitting (with rotation angles $X = -57° \pm 2°$ and $Y = 9° \pm 3$), but the two geometries cannot be distinguished anyway without the use of an enantiomerically labeled retinal. Since the three deuteromethyl group bond vectors on the tetrahedral unit are related by a 3-fold symmetry axis, the identified cyclohexene ring structure may be expected to exhibit a 3-fold redundancy. However, this redundancy is lifted as a result of the differing spectral intensities of the deuteromethyl groups. The two CD_3 groups and the CD_2H group contribute in a ratio of 3:3:2 to the spectrum and may therefore be distinguished since any permutation of the components in the simulation has a distinct effect on the quality of the line fit.

The rotations $X = -33°$ and $Y = 9°$ are now performed on the three unit vectors from their starting positions, to yield the coordinates $\{x,y,z\}$ for the three deuteromethyl groups on the cyclohexene ring of retinal:

$$CD_3 \text{ vector (a)} = \{-0.60, -0.80, -0.08\}$$

$$CD_3 \text{ vector (b)} = \{-0.54, 0.80, 0.26\}$$

$$CD_2H \text{ vector} = \{0.70, -0.17, 0.70\}$$

The cone angle γ of any methyl group is defined by the cosine of the z-component of its chemical bond vector, and thus the three methyl rotor angles relative to the membrane normal are found:

$$CD_3 \text{ angle (a)} = 95° \pm 2°$$

$$CD_3 \text{ angle (b)} = 75° \pm 2°$$

$$CD_2H \text{ angle} = 46° \pm 3°$$

It is apparent that the angles of the two CD_3 groups on the cyclohexene ring are indeed close to 90°, as had been qualitatively concluded earlier, so they lie approximately horizontal in the membrane.

Figure 6 illustrates how the three methyl groups contribute to the ^2H NMR spectrum at a horizontal sample inclination (α = 0°). The top spectrum [expanded from Figure 4(ii)] is shown with its best-fit line shape simulation superimposed. The simulation underneath was generated with the same X and Y values, but using a zero intrinsic line width and a zero mosaic spread. Thus the effects of line broadening have been removed artificially to reveal the underlying peak positions and the values of the three quadrupole splittings. The two CD_3 groups and the CD_2H group are recognized by their relative peak intensities. Since the ζ_+ and ζ_- transitions of the deuterium nucleus are distinguished in the line shape calculation, even the signs of the three quadrupole splittings are available from the simulation output shown in Figure 6:

$$\Delta\nu_Q = -39 \text{ kHz}$$

$$\Delta\nu_Q = -32 \text{ kHz}$$

$$\Delta\nu_Q = +18 \text{ kHz}$$

Note that these values of $\Delta\nu_Q$ are related to the cone angles γ via eq 1 (with $\theta = \gamma$) and that they are necessarily consistent with the bond vectors given above.

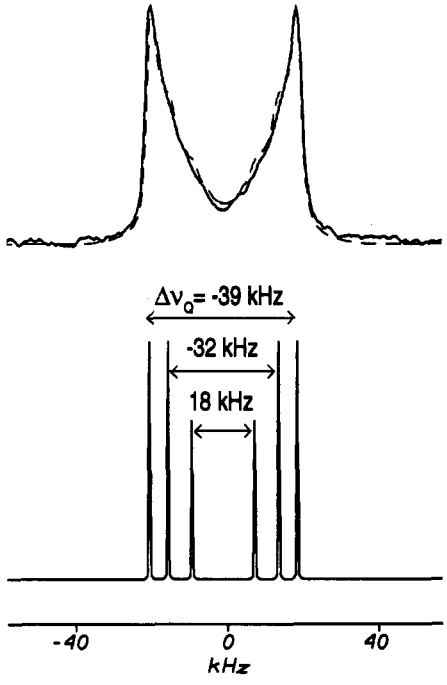

FIGURE 6: ^{2}H NMR spectrum from Figure 4(ii) at $\alpha = 0°$, in which the three contributing spectral components are not resolved. The experimental spectrum of BR (upper, solid line) is shown with the line shape simulation superimposed (dashed line). Below, an equivalent simulation is generated with the same X and Y values, but with zero intrinsic line width and zero mosaic spread to reveal the underlying peak positions and quadrupole splittings $\Delta\nu_Q$.

If overlap would not have constituted a problem, or if, for example, only a single deuteromethyl group had been labeled at a time, the whole simulation analysis would not have been essential. According to the basic strategy of this ^{2}H NMR method, the angle γ of a deuteromethyl group would then be obtained directly from the quadrupole splitting $\Delta\nu_Q$ using eq 1 (with $\theta = \gamma$). The sign of the splitting would be concluded from the spectrum at a sample inclination $\alpha = 90°$, or the correct angle could be chosen by the use of a restriction plot depicting the possible combinations with other known angles such that they are consistent with the geometry of the deuterated site.

DISCUSSION

From a tilt series of ^{2}H NMR spectra recorded with a uniaxially oriented sample at different inclinations in the magnetic field, it has been possible to evaluate the bond vectors of three labeled methyl groups on the cyclohexene ring of retinal in bacteriorhodopsin. In Figure 7, these three orientations are used as geometrical constraints to build the molecular framework relative to the membrane surface which lies in the x–y plane. Many important features of the structure and geometry of the cyclohexene ring and even of the whole chromophore can be deduced qualitatively by inspection of this picture.

Although the three methyl groups lie fixed in the membrane, the absolute conformation within the irregularly puckered ring is not precisely defined. There remains a degree of intramolecular flexibility in the form of a skew of the rigid C_5–C_7 unit about the C_1–C_6 bond, which is illustrated in Figure 7 (but note that the tetrahedral symmetry between the three deuteromethyl groups is always retained). Nevertheless, for moderate skew angles the average plane through the puckered cyclohexene ring is roughly defined by the orientation of the CD_2H group or by the plane bisecting the angle between the

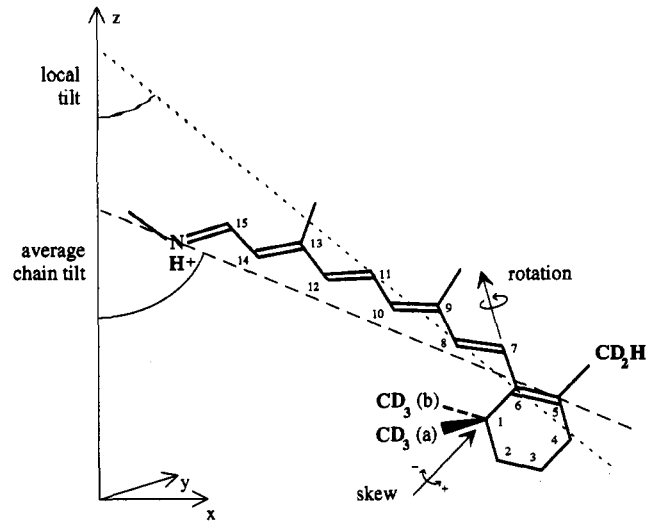

FIGURE 7: Three-dimensional structure of the cyclohexene ring of retinal in BR as determined by ^{2}H NMR, relative to the membrane surface in the x–y plane. Analysis of the orientations of the three deuteromethyl groups on the puckered ring (skew around C_1–C_6) indicates that the chromophore has a (6S)-trans conformation around the C_6–C_7 bond. The reference axis defined by carbons C_4 and C_6 (dotted line) gives a local tilt angle at the cyclohexene ring which differs from that of the average end-to-end chromophore long axis (dashed line) due to an in-plane curvature of the polyene chain.

two CD_3 groups which are approximately horizontal in the membrane. Therefore, the cyclohexene ring must be aligned nearly vertical within the protein.

The polyene chain can make any angle around the C_6–C_7 bond, because of the shallow potential well associated with this rotation (Warshel & Karplus, 1974). Therefore, in principle, a retinal conformation anywhere beteen (6S)-trans and (6S)-cis would be possible. However, in BR the molecular plane of the polyene chain is known to lie approximately vertical in the membrane (Earnest et al., 1986; Urabe et al., 1989; Lin & Mathies, 1989) as does the cyclohexene ring as shown above. Therefore, the whole chromophore must be essentially planar. A rotation in Figure 7 of the polyene chain by 180° would place it almost perpendicular to the membrane plane, and such a (6S)-cis conformation is clearly incompatible with the recognized average chain tilt near 67° (Heyn et al., 1977; Korenstein & Hess, 1978; Bamberg et al., 1979; Barabas et al., 1983; Earnest et al., 1986; Urabe et al., 1989; Lin & Mathies, 1989; Schertler et al., 1991). The plausible structure in our model must therefore be close to (6S)-trans, which had been suggested for retinal within BR (Harbison et al., 1985; van der Steen et al., 1986; Smith et al., 1989; Copie et al., 1990) and has recently been confirmed by rotational resonance ^{13}C NMR (Creuzet et al., 1991).

Having identified the orientation of the cyclohexene ring as well as the intramolecular conformation of retinal, it is now possible to estimate the angle of inclination for the polyene chain. In the case of a perfectly planar (6S)-trans conformation, the chromophore long axis could simply be represented by the extended conjugated system which makes a fixed 90° angle to the CD_2H group. The local tilt angle at the cyclohexene ring is thus conveniently definedthrough carbons C_4 and C_6, shown as the dotted line in Figure 7. The angle of this local reference axis relative to the membrane normal is calculated to be approximately 47° for the case that there is no skew around the C_1–C_6 bond in the cyclohexene ring. Allowing for the intramolecular puckering of the ring, there exists a smooth but very limited range of theoretical tilt angles which are compatible with the initial constraints on the three

deuteromethyl groups. Nevertheless, in any case the local cyclohexene tilt angle represented by our reference axis (dotted line through carbons C_4 and C_6 in Figure 7) is found to be considerably steeper than the known average retinal tilt near 67° (dashed line) as determined by spectroscopic methods (Heyn et al., 1977; Korenstein & Hess, 1978; Bamberg et al., 1979; Barabas et al., 1983; Earnest et al., 1986; Lin & Mathies, 1989; Schertler et al., 1991) or 65° ± 12° from neutron diffraction studies (Hauss et al., 1990). It is seen in Figure 7 that, by the way the polyene chain is attached to the fixed cyclohexene ring, it cannot be brought any closer to the expected tilt (dashed line) of the chromophore long axis, even by rotating it around the C_6–C_7 bond. We therefore conclude that the polyene chain must be slightly curved, since the other structural methods quoted above have resolved the *average* chain orientation. Such an in-plane bending has been suggested previously as a possible explanation for a set of NMR chemical shielding tensors of ^{13}C-labeled retinal in BR (Harbison et al., 1984b). The curvature of retinal analogues is directly recognizable in the crystal structures of a retinol binding protein (Newcomer et al., 1984) and a photoreceptor protein (McRee et al., 1989), and it is commonly found in single crystals of *all-trans*-(6*S*)-retinal derivatives and other carotenoids (Stam, 1972; Drikos et al., 1988; Santasiero et al., 1990). This distortion of the conjugated system probably relieves steric crowding of the methyl groups along the chain, which can be demonstrated theoretically by an energy minimization of the molecular framework producing the expected curvature [for a representative picture, see Lin and Mathies (1989)]. In all cases of a bent retinal structure, the curvature accounts for a difference of at least 10° in the angle between the average chromophore long axis and the local reference that describes the tilt at the cyclohexene ring.

Another additional reason for the difference in tilt angles between our findings and previous reports could be due to an off-axis orientation of the electronic transition moment, which is the property detected by optical spectroscopy [as used by Heyn et al. (1977), Korenstein and Hess (1978), Bamberg et al. (1979), Barabas et al. (1983), Lin and Mathies (1989), and Schertler et al. (1991)]. Such a deviation has recently been demonstrated for a representative conjugated polyene (Shang et al., 1991), where the transition moment was found to be inclined away from the long axis of the molecule by 15° in the direction of the double bonds. Drikos and Rüppel (1984) established the alignment of the transition moment in crystalline (6*S*)-*cis*-retinal with an all-trans chain relative to the curved molecular framework, and a similar small deviation from the end-to-end axis is recognized. These observations imply that the average chromophore tilt is indeed steeper than has previously been assumed from spectroscopic studies and thus even closer to our local tilt axis. Further information on the bending or even twisting of the polyene chain may be obtained by ^2H NMR experiments with deuterated methyl groups at positions C_9 and C_{13} on retinal.

It is seen that in this coordinate system the whole chromophore must be tilted *downward* from the Schiff base, with the methylene carbons on the ring portion C_1–C_4 pointing further down. Independent studies have shown that retinal is inclined toward the extracellular side of BR (Huang et al., 1982; Huang & Lewis, 1989), which thus defines the absolute sidedness of the protein in our frame of reference. Consequently, the methyl groups attached to carbons C_5, C_9, and C_{13} point up toward the cytoplasmic side (Lin & Mathies, 1989; Hauss et al., 1990), and the proton on the Schiff base thus faces downward. This is the case for both the all-trans and the 13-cis form of retinal which make up the dark-adapted state of BR, since thermal isomerization occurs via a concerted "pedal" mechanism in which the C_{15}=N double bond also flips (Smith et al., 1984; Harbison et al., 1984a). Our spectral simulations have shown that the orientation of the labeled molecular unit is sufficiently well defined to exclude the possibility of a significant change in local geometry upon thermal isomerization. This observation is supported by Schertler et al. (1991), who measured a difference of <0.4° between the transition moments of the light- and the dark-adapted states of BR. During the photocycle, on the other hand, considerable structural changes occur both in the chromophore and in the protein. Trapping of photocycle intermediates and observation of the chromophore geometry by ^2H NMR might provide further details toward the characterization of protein function.

All the results presented here are based on a direct determination of the orientations of specific molecular segments of a protein-bound prosthetic group, and the conclusions could be derived ab initio by solid-state NMR without recourse to any other information on the system. We are therefore confident that this ^2H NMR method promises some general application in noncrystallographic structural studies of membrane proteins, particularly of those with an easily accessible prosthetic group or with amino acid side chains that can be labeled.

ACKNOWLEDGMENT

We thank Ingrid Wallat (Freie Universität, Berlin) for preparation of the sample and Dr. C. Dobson (ICL, Oxford) for the use of the Bruker MSL 200.

REFERENCES

Bamberg, E., Apell, H.-J., Dencher, N. A., Sperling, W., Stieve, H., & Läuger, P. (1979) *Biophys. Struct. Mech. 5*, 277–292.

Barabas, K., Der, A., Dancshazy, Z., Ormos, P., Keszthelyi, L., & Marden, M. (1983) *Biophys. J. 43*, 5–11.

Beshah, K., Olejniczac, E. T., & Griffin, R. G. (1987) *J. Chem. Phys. 86*, 4730–4736.

Ceska, T. A., & Henderson, R. (1990) *J. Mol. Biol. 213*, 539–560.

Clark, N. A., Rothschild, K. J., Luippold, D. A., & Simon, B. A. (1980) *Biophys. J. 31*, 65–96.

Copie, V., McDermott, A., Beshah, K., Spijker, M., Lugtenburg, J., Herzfeld, J., & Griffin, R. G. (1990) *Biophys. J. 57*, 360a.

Creuzet, F., McDermott, A., Gebhard, R., van der Hoef, K., Spijker-Assink, M. B., Herzfeld, J., Lugtenburg, J., Levitt, M. H., & Griffin, R. G. (1991) *Science 251*, 783–786.

Drikos, G., Dietrich, H., & Rüppel, H. (1984) *Photochem. Photobiol. 40*, 93–104.

Drikos, G., Dietrich, H., & Rüppel, H. (1988) *Eur. Biophys. J. 16*, 193–205.

Earnest, T. N., Roepe, P., Braiman, M. S., Gillespie, K. J., & Rothschild, J. (1986) *Biochemistry 25*, 7793–7798.

Ekiel, I., Marsh, D., Smallbone, B. W., Kates, M., & Smith, I. C. P. (1981) *Biochem. Biophys. Res. Commun. 100*, 105–110.

Griffin, R. G., Beshah, K., Ebelhäuser, R., Huang, E. T., Olejniczak, E. T., Rice, D. M., Siminovitch, D. J., & Wittebort, R. J. (1988) in *The Time Domain in Surface and Structural Dynamics* (Long, G. J., & Grandjean, F., Eds.) pp 81–105, Kluwer Academic Publishers, Dordrecht, The Netherlands.

Harbison, G. S., Smith, S. O., Pardoen, Mulder, P. J., Lugtenburg, J., Herzfeld, J., Mathies, R., & Griffin, R. G. (1984a) *Biochemistry 23*, 2662–2667.

Harbison, G. S., Smith, S. O., Pardoen, J. A., Winkel, C., Lugtenburg, J., Herzfeld, J., Mathies, R., & Griffin, R. G. (1984b) *Proc. Natl. Acad. Sci. U.S.A. 81*, 1706–1709.

Hauss, T., Grzesiek, S., Otto, H., Westerhausen, J., & Heyn, M. P. (1990) *Biochemistry 29*, 4904–4913.
Henderson, R., Baldwin, J. M., Ceska, T. A., Zemlin, F., Beckmann, E., & Downing, K. H. (1990) *J. Mol. Biol. 213*, 899–929.
Heyn, M. P., Cherry, R. J., & Müller (1977) *J. Mol. Biol. 117*, 607–620.
Heyn, M. P., Westerhausen, J., Wallat, I., & Seiff, F. (1988) *Proc. Natl. Sci. U.S.A. 85*, 2146–2150.
Huang, J. Y., & Lewis, A. (1989) *Biophys. J. 55*, 835–842.
Huang, K. S., Radhakrishnam, R., Bayley, H., & Khorana, H. G. (1982) *J. Biol. Chem. 257*, 13616–13623.
Kates, K., Kushwaha, S. C., & Sprott, G. D. (1982) *Methods Enzymol. 88*, 98–105.
Korenstein, R., & Hess, B. (1978) *FEBS Lett. 89*, 15–20.
Kouyama, T., Kimura, Y., Kinosita, K., & Ikegami, A. (1981) *FEBS Lett. 124*, 100–104.
Lee, R. W. K., & Oldfield, E. (1982) *J. Biol. Chem. 257*, 5023–5029.
Lin, S. W., & Mathies, R. A. (1989) *Biophys. J. 56*, 653–660.
Lugtenburg, J., Mathies, R. A., Griffin, R. G., & Herzfeld, J. (1988) *Trends Biochem. Sci. 13*, 388–393.
Mathies, R. A., Lin, S. W., Ames, J. B., & Pollard, W. T. (1991) *Annu. Rev. Biophys. Chem. 20*, 491–518.
McRee, D. E., Tainer, J. A., Meyer, T. E., Van Beeumen, J., Cusanovich, M. A., & Getzoff, E. D. (1989) *Proc. Natl. Acad. Sci. U.S.A. 86*, 6533–6537.
Newcomer, M. E., Jones, T. A., Aqvist, J., Sundelin, J., Eriksson, U., Rask, L., & Petersen, P. A. (1984) *EMBO J. 3*, 1451–1454.
Opella, S. J. (1990) in *Biological Magnetic Resonance* (Berliner, L. J., & Reuben, J., Eds.) Vol. 9, pp 177–197, Plenum Press, New York.
Santasiero, B. D., James, M. N. G., Mahendran, M., & Childs, R. F. (1990) *J. Am. Chem. Soc. 112*, 9416–9418.
Schertler, G. F. X., Lozier, R., Michel, H., & Oesterhelt, D. (1991) *EMBO J. 10*, 2353–2361.
Seelig, J. (1977) *Q. Rev. Biophys. 10*, 353–418.
Seelig, J. (1978) *Biochim. Biophys. Acta 515*, 105–140.
Seiff, F., Westerhausen, J., Wallat, I., & Heyn, M. P. (1986) *Proc. Natl. Acad. Sci. U.S.A. 83*, 7746–7750.
Seiff, F., Westerhausen, J., Wallat, I., & Heyn, M. P. (1987) in *Receptors and Ion Channels* (Ovchinnikov, Y. A., & Hucho, F., Eds.) pp 255–263, de Gruyter, Berlin.
Shang, Q.-y., Dou, X., & Hudson, B. S. (1991) *Nature 352*, 703–705.
Shon, K.-J., Kim, Y., Colnago, L. A., & Opella, S. J. (1991) *Science 252*, 1303–1308.
Smith, R. L., & Oldfield, E. (1984) *Science 225*, 280–288.
Smith, S. O., Myers, A. B., Pardoen, J. A., Winkel, C., Mulder, P. P. J., Lugtenburg, J., & Mathies, R. (1984) *Proc. Natl. Acad. Sci. U.S.A. 81*, 2055–2059.
Smith, S. O., de Groot, H. J. M., Gebhard, R., Courtin, J. M. L., Lugtenburg, J., Herzfeld, J., & Griffin, R. G. (1989) *Biochemistry 28*, 8897–8904.
Stam, C. H. (1972) *Acta Crystallogr. B28*, 2936–2945.
Ulrich, A. S., & Watts, A. (1991) in *Dynamics of Membrane Assembly* (Op den Kamp, J. A. F., Ed.) NATO ASI Series, Springer-Verlag, Berlin.
Urabe, H., Otomo, J., & Ikegami, A. (1989) *Biophys. J. 56*, 1225–1228.
van der Steen, R., Biesheuvel, P. L., Mathies, R. A., & Lugtenburg, J. (1986) *J. Am. Chem. Soc. 108*, 6410–6411.
Vaz, N. A., Vaz, M. J., & Doane, J. W. (1984) *Phys. Rev. A 30*, 1008–1016.
Warshel, A., & Karplus, M. (1974) *J. Am. Chem. Soc. 96*, 5677–5689.

Registry No. Retinal, 116-31-4.